

New potential antitumoral fluorescent tetracyclic thieno[3,2-*b*]pyridine derivatives: interaction with DNA and nanosized liposomes

Elisabete M. S. Castanheira^{*1}, Maria Solange D. Carvalho^{1,2}, Ana Rita O. Rodrigues¹, Ricardo C. Calhelha², and Maria-João R. P. Queiroz²

¹Centre of Physics (CFUM), University of Minho, Campus de Gualtar, Braga, 4710-057, Portugal

²Centre of Chemistry (CQ-UM), University of Minho, Campus de Gualtar, Braga, 4710-057, Portugal

^{*}Corresponding author

Abstract

Fluorescence properties of two new potential antitumoral tetracyclic thieno[3,2-*b*]pyridine derivatives were studied in solution and in liposomes of DPPC (dipalmitoyl phosphatidylcholine), egg lecithin (phosphatidylcholine from egg yolk; Egg-PC) and DODAB (dioctadecyldimethylammonium bromide). Compound **1**, pyrido[2',3':3,2]thieno[4,5-*d*]pyrido[1,2-*a*]pyrimidin-6-one, exhibits reasonably high fluorescence quantum yields in all solvents studied ($0.20 \leq \Phi_F \leq 0.30$), while for compound **2**, 3-[(*p*-methoxyphenyl)ethynyl]pyrido[2',3':3,2]thieno[4,5-*d*]pyrido[1,2-*a*]pyrimidin-6-one, the values are much lower ($0.01 \leq \Phi_F \leq 0.05$). The interaction of these compounds with salmon sperm DNA was studied using spectroscopic methods, allowing the determination of intrinsic binding constants, $K_i = (8.7 \pm 0.9) \times 10^3 \text{ M}^{-1}$ for compound **1** and $K_i = (5.9 \pm 0.6) \times 10^3 \text{ M}^{-1}$ for **2**, and binding site sizes of $n = 11 \pm 3$ and $n = 7 \pm 2$ base pairs, respectively. Compound **2** is the most intercalative compound in salmon sperm DNA (35%), while for compound **1** only 11% of the molecules are intercalated. Studies of incorporation of both compounds in liposomes of DPPC, Egg-PC and DODAB revealed that compound **2** is mainly located in the hydrophobic region of the lipid bilayer, while compound **1** prefers a hydrated and fluid environment.

Introduction

Liposomes are among technological delivery developments for chemotherapeutic drugs in the treatment of cancer. This technique can potentially overcome many common pharmacologic problems, such as those involving solubility, pharmacokinetics, in vivo stability and toxicity [1-3]. Liposomes are closed spherical vesicles consisting of a lipid bilayer that encapsulates an aqueous phase in which hydrophilic drugs can be stored, while water insoluble compounds can be incorporated in the hydrophobic region of the lipid bilayer [4].

In this work, two new potential antitumoral fluorescent planar tetracyclic thieno[3,2-*b*]pyridine derivatives **1** and **2** (Figure 1), previously synthesized by some of us [5], were encapsulated in

liposomes of DPPC (dipalmitoyl phosphatidylcholine), egg lecithin (phosphatidylcholine from egg yolk) and DODAB (dioctadecyldimethylammonium bromide). DPPC and egg lecithin [egg yolk phosphatidylcholine (Egg-PC)] are neutral components of biological membranes, while cationic liposomes based on the synthetic lipid DODAB have been used as vehicles for DNA transfection and drug delivery [6]. These studies are important keeping in mind future drug delivery applications using these compounds as anticancer drugs.

Due to the antitumoral potential of the two compounds **1** and **2**, related with their possible intercalation between the DNA base pairs, interactions with natural double-stranded salmon sperm DNA were studied. These interactions can be assessed using spectroscopic measurements, which are important tools for monitoring DNA-binding processes. The investigation based on DNA interactions has a key importance in order to understand the mechanisms of action of antitumor and antiviral drugs and to design new DNA-targeted drugs [7, 8]. Small molecules are stabilized on groove binding and intercalation with DNA through a series of associative interactions such as π -stacking, hydrogen bonding, attractive van der Waals and hydrophobic interactions [8]. The occurrence of intercalation seems to be an essential (but not sufficient) step for antitumoral activity [7]. Fluorescence quenching experiments using external quenchers are also very useful to distinguish between DNA binding modes [9] since intercalated molecules are less accessible to anionic quenchers due to electrostatic repulsion with negatively charged DNA [10].

Experimental

Salmon sperm DNA from Invitrogen (Carlsbad, CA, USA) and compounds stock solutions were prepared in 10 mM Tris-HCl buffer (pH = 7.4), with 1 mM EDTA. The DNA concentration in number of bases was determined from the molar absorption coefficient, $\epsilon = 6600 \text{ M}^{-1} \text{ cm}^{-1}$ at 260 nm [11]. Fluorescence spectra of several solutions with different [DNA]/[compound] ratios and constant compound concentration ($5 \times 10^{-6} \text{ M}$) were recorded. The solutions were left several hours to stabilize. Dipalmitoyl phosphatidylcholine (DPPC), egg yolk phosphatidylcholine (Egg-PC), from Sigma-Aldrich (St. Louis, Missouri, USA), and dioctadecyldimethylammonium bromide (DODAB), from Tokyo Kasei (Tokyo, Japan), were used as received. Liposomes were prepared by the ethanolic injection method, previously used for the preparation of Egg-PC and DPPC liposomes [12-15] and DODAB vesicles [16, 17]. An ethanolic solution of a lipid/compound mixture was injected in an aqueous buffer solution under vigorous stirring, above the melting transition temperature of the lipid (approx. 41°C for DPPC [18] and 45°C for DODAB [19]). The final lipid concentration was 1 mM, with a compound/lipid molar ratio of 1:500. One millilitre solutions of liposome dispersions were placed in 3 mL disposable polystyrene cuvettes for dynamic light scattering (DLS) measurements in a Malvern ZetaSizer Nano ZS particle analyzer (Worcestershire, UK). Five independent measurements were performed for each sample. Malvern Dispersion Technology Software (DTS) (Worcestershire,

UK) was used with multiple narrow mode (high resolution) data processing, and mean size (nm) and error values were considered.

Absorption spectra were recorded in a Shimadzu UV-3101PC UV-Vis-NIR spectrophotometer (Kyoto, Japan) and fluorescence measurements were obtained in a Fluorolog 3 spectrofluorimeter (HORIBA Scientific, Kyoto, Japan) equipped with Glan-Thompson polarizers. Fluorescence spectra were corrected for the instrumental response of the system. The fluorescence quantum yields were determined by the standard method [20, 21], using 9,10-diphenylanthracene in ethanol as reference, $\Phi_F = 0.95$ [22]. The solutions were previously bubbled for 20 min with ultrapure nitrogen.

Results and discussion

The size and size distribution of the liposomes prepared was obtained by DLS. All the liposomes have a mean hydrodynamic radius lower than 150 nm and generally low polydispersity. For Egg-PC and DODAB liposomes, the size distributions are bimodals and broader than for DPPC liposomes, the Egg-PC being the more polydisperse (Figure 2). The ethanolic injection method was described to produce phospholipid small unilamellar vesicles (SV) [12-15]. Accordingly, DPPC and Egg-PC liposomes obtained here are in this category, with a mean diameter of around 90 nm for DPPC and 50 nm for Egg-PC. DODAB liposomes exhibit a significantly larger mean diameter (around 270 nm) than the phospholipid ones. The size of DODAB vesicles strongly depends on the preparation method, sonication and ethanolic injection giving small DODAB vesicles [17, 23, 24], while injection using chloroform yielded large DODAB vesicles [16]. Besides, spontaneously prepared DODAB liposomes have a much larger size (hydrodynamic radius around 337 nm [25]), being considered giant unilamellar vesicles (GUV). The DODAB liposomes mean diameter obtained here (*ca.* 270 nm) compares well with the reported value of 249 nm for DODAB SV [16]. In all samples, no experimental evidence of the presence of open bilayer fragments (diameter lower than 10 nm [17]) was obtained (Figure 2).

The absorption and fluorescence properties of compounds **1** and **2** were studied in several solvents (Table 1). The normalized fluorescence spectra of compounds **1** and **2** are shown in Figures 3 and 4. The fluorescence emission maximum of both compounds displays a loss of vibrational structure in polar solvents together with a small red shift (Figures 3 and 4), indicating some charge transfer character of the excited state [26]. The red shifts are more significant for compound **2** (Table 1), which may be due to a higher capability of this compound to establish hydrogen bonds with protic solvents (especially with water), due to the presence of the OCH₃ group. Compound **1** has significantly higher fluorescence quantum yields (between 20 and 30%) than compound **2** (Φ_F between 1 and 5%), showing that the functionalization of the pyridine ring with a triple bond linked to a *p*-methoxyphenyl group causes a significant enhance of the non-radiative deactivation pathways. The fluorescence

quantum yields of compound **1** are also higher than the ones of a benzo[*b*]thiophene derivative of the same type, a benzothienopyridopyrimidone [27], in which the benzene ring linked to the thiophene is substituted in compound **1** by a pyridine ring. The intrinsic fluorescence of compounds **1** and **2** can be used to monitor interactions with DNA and compounds behaviour when encapsulated in liposomes.

Both compounds **1** and **2** were tested for their interaction with natural salmon sperm DNA using spectroscopic methods. For compound **1**, fluorescence intensity decreases with increasing DNA concentration, while the opposite happens for compound **2** (Figures 5 and 6). This behaviour, also previously observed for differently substituted tetracyclic lactams [28], may indicate a different type of interaction of both compounds with the DNA molecule. For the two compounds, full saturation (corresponding to spectral invariance with increasing DNA concentration) is attained at [DNA]/[compound] = 200, meaning that total binding is achieved at this ratio. The high [DNA]/[compound] ratio needed for total binding, together with the negligible changes observed in absorption spectra (not shown), point to a weak interaction of these molecules with the nucleic acid.

The intrinsic binding constants (K_i) and binding site sizes (n) were determined (Table 2) through the McGhee and von Hippel modification of Scatchard plot (Equation 1) [29],

$$\frac{r}{c_f} = K_i (1 - nr) \left[\frac{(1 - nr)}{(1 - (n-1)r)} \right]^{n-1} \quad (1)$$

where K_i is the intrinsic binding constant, n the binding site size, r the ratio $c_b/[DNA]$ and c_b and c_f the concentrations of bound and free compound, respectively, calculated by

$$c_b = \frac{I_{F,0} - I_F}{I_{F,0} - I_{F,b}} \times c_{\text{total}}; \quad c_{\text{total}} = c_f + c_b \quad (2)$$

being $I_{F,0}$ the fluorescence intensity of the free compound and $I_{F,b}$ the fluorescence intensity of the bound compound at total binding. The binding constants (Table 2) are moderately low, with a large number of base pairs between consecutive intercalated compound molecules (n).

Anionic quenchers can be useful in distinguishing between DNA binding modes [9, 10]. Compounds that are bound at the DNA surface (groove binding or electrostatic binding) are more accessible and emission from these molecules can be quenched more efficiently. Fluorescence quenching measurements using iodide ion showed that the usual Stern–Volmer plots (plots of the fluorescence intensity ratio in the absence, I_0 , and presence, I , of quencher vs. quencher concentration) are not linear and exhibit a downward curvature (Figure 7A). This indicates that some compound molecules are not accessible to the anionic quencher, being intercalated between DNA base pairs. The modified Stern–Volmer plot [30] (Equation 3) allows the determination of the fraction of compound molecules accessible to quencher,

$$\frac{I_0}{\Delta I} = \frac{1}{f_a} + \frac{1}{f_a K_{sv} [Q]} \quad (3)$$

where I_0 is the fluorescence intensity in the absence of quencher, $\Delta I = I_0 - I$, K_{SV} the Stern–Volmer constant, $[Q]$ the quencher concentration and f_a the fraction of molecules accessible to quencher.

The representations of the modified Stern–Volmer plot are reasonably linear (Figure 7B) and the f_a values are in Table 2. Both compounds exhibit some intercalation in DNA, compound **2** being the more intercalative one, with a lower fraction (65%) of molecules accessible to anionic quencher. The higher hydrophobic character of compound **2**, promoted by the functionalization of the pyridine with a triple bond linked to a *p*-methoxyphenyl group, may justify this behaviour. As both compounds **1** and **2** are neutral molecules (and electrostatic interaction with the negatively charged DNA molecule is not expected), the high f_a values indicate that the main type of interaction with the nucleic acid must be the binding to DNA grooves [28].

Fluorescence experiments of both compounds encapsulated in liposomes of DPPC, DODAB and Egg-PC were carried out (Figure 8), in both gel (below T_m) and liquid-crystalline (above T_m) phases. The melting transition temperature of Egg-PC is very low [31] and this lipid is in the fluid liquid-crystalline phase at room temperature. Fluorescence spectra of compound **1** incorporated in liposomes (Figure 8, Table 3) are roughly similar to the one obtained in pure water, regarding the band shape and maximum emission wavelength. Compound **2** in liposomes presents emission spectra similar to those in polar solvents, significantly blue-shifted relative to water. In Egg-PC, a band enlargement is observed in the blue region, which can indicate two different locations of compound **2** in these liposomes, one deep in the hydrophobic region and another more close to the lipid polar heads.

Fluorescence anisotropy (r) measurements (Table 3) can give relevant information about the location of the compounds in liposomes, as r increases with the rotational correlation time of the fluorescent molecule (and, thus, with the viscosity of the fluorophore environment) [26]. Anisotropy values in a viscous solvent (glycerol) were also determined, for comparison. Anisotropy results (Table 3) allow to conclude that compound **2** is mainly located in the inner region of the lipid bilayer, feeling the penetration of some water molecules. The transition from the rigid gel phase to the liquid-crystalline phase is clearly detected by a significant decrease in anisotropy at 55°C observed in DPPC and DODAB liposomes. Compound **1** exhibits a different behaviour and anisotropy is very low in all types of liposomes (and much lower than in glycerol, Table 3). Overall, the results indicate that compound **1** prefers a hydrated and fluid environment and the transition from the gel phase to the liquid-crystalline phase is not detected. To further clarify the location of compound **1**, the solutions of liposomes with incorporated compound were passed through filters of 0.05 μm diameter. The fluorescence emission of the filtered solutions was negligible, indicating that compound **1** is mainly in the liposome aqueous interior or located at the interfaces, with a very hydrated environment. This behaviour is similar to the observed previously for a benzothienopyridopyrimidone in lipid vesicles [27]. The encapsulation

assays performed here may be important for future drug delivery applications of these potential antitumoral compounds using liposomes as drug carriers.

Conclusions

The interaction with DNA of two new potential antitumoral fluorescent planar thieno[3,2-*b*]pyridine derivatives was studied using spectroscopic methods. Compound **2** was shown to be the most intercalative compound in salmon sperm DNA (35%). The binding to DNA grooves seems to be the main type of interaction with the nucleic acid. Studies of incorporation of both compounds in liposomes of DPPC, Egg-PC and DODAB revealed that compound **2** is mainly located in the hydrophobic region of the lipid bilayer, while compound **1** prefers a hydrated and fluid environment. Our data thus suggest that both potential antitumoral compounds may be transported in liposomes for drug delivery applications.

Abbreviations

DLS, dynamic light scattering; DODAB, dioctadecyldimethylammonium bromide; DPPC, dipalmitoyl phosphatidylcholine; DTS, Dispersion Technology Software; Egg-PC, egg yolk phosphatidylcholine; GUV, giant unilamellar vesicles; SV, small unilamellar vesicles.

Competing interests

The authors declare that they have no competing interests.

Authors' contributions

EMSC conceived the study, was responsible for its coordination and for the interpretation of results, and drafted the manuscript. MSDC carried out the liposome preparation and the fluorescence studies in liposomes. AROR carried out the experimental studies of the compounds interaction with DNA. RCC carried out the synthesis, purification and characterization of the new compounds. MJRPQ supervised the organic synthesis and participated in the draft of the manuscript. All authors read and approved the final manuscript.

Acknowledgements

This work was funded by FCT-Portugal through CFUM, CQ-UM, Project PTDC/QUI/81238/2006 (cofinanced by program FEDER/COMPETE, ref. FCOMP-01-0124-FEDER-007467) and PhD grants of M.S.D. Carvalho (SFRH/BD/47052/2008) and R.C. Calhelha (SFRH/BD/29274/2006).

References

1. Andresen TL, Jensen SS, Jorgensen K: **Advanced strategies in liposomal cancer therapy: Problems and prospects of active and tumor specific drug release.** *Prog Lipid Res* 2005, **44**:68.
2. Ocheke NA, Olorunfemi PO, Ngwuluka NC: **Nanotechnology and drug delivery. Part 1: Background and applications.** *Tropical J Pharm Res* 2009, **8**:265.
3. Ocheke NA, Olorunfemi PO, Ngwuluka NC: **Nanotechnology and drug delivery. Part 2: Nanostructures for Drug Delivery.** *Tropical J Pharm Res* 2009, **8**:275.
4. Malam Y, Loizidou M, Seifalian AM: **Liposomes and nanoparticles: nanosized vehicles for drug delivery in cancer.** *Trends Pharmacol Sci* 2009, **30**:592.
5. Calhelha RC, Queiroz M-JRP: **Synthesis of new thieno[3,2-*b*]pyridine derivatives by palladium-catalyzed couplings and intramolecular cyclizations.** *Tetrahedron Lett* 2010, **51**:281.
6. Pedroso de Lima MC, Simões S, Pires P, Faneca H, Düzgünes N: **Cationic lipid-DNA complexes in gene delivery: from biophysics to biological applications.** *Adv Drug Deliv Rev* 2001, **47**:277.
7. Lyne PD: **Structure-based virtual screening: an overview.** *Drug Discovery Today* 2002, **7**:1047.
8. Mahadevan S, Palaniandavar M: **Spectroscopic and voltammetric studies of copper(II) complexes of bis(pyrid-2-yl)-di/trithia ligands bound to calf thymus DNA.** *Inorg Chim Acta* 1997, **254**:291.
9. Kumar CV, Asuncion EH: **DNA-binding studies and site-selective fluorescence sensitization of an anthryl probe.** *J Am Chem Soc* 1993, **115**:8547.
10. Kumar CV, Punzalan EHA, Tan WB: **Adenine-thymine base pair recognition by an anthryl probe from the DNA minor groove.** *Tetrahedron* 2000, **56**:7027.
11. Renault E, Fontaine-Aupart MP, Tfibel T, Gardes-Albert M, Bisagni E: **Spectroscopic study of the interaction of pazelliptine with nucleic acids.** *J Photochem Photobiol B Biol* 1997, **40**:218.
12. Batzri S, Korn ED: **Single bilayer liposomes prepared without sonication.** *Biochim Biophys Acta* 1973, **298**:1015.
13. Kremer JMH, Esker MWJvd, Pathmamanoharan C, Wiersema PH: **Vesicles of variable diameter prepared by a modified injection method.** *Biochemistry* 1977, **16**:3932.
14. Nordlund JR, Schmidt CF, Dicken SN, Thompson TE: **Transbilayer distribution of phosphatidylethanolamine in large and small unilamellar vesicles.** *Biochemistry* 1981, **20**:3237.
15. Cruz A, Casals C, Plasencia I, Marsh D, Pérez-Gil J: **Depth profiles of pulmonary surfactant protein B in phosphatidylcholine bilayers, studied by fluorescence and electron spin resonance spectroscopy.** *Biochemistry* 1998, **37**:9488.
16. Tsuruta LR, Carmona-Ribeiro AM: **Counterion effects on colloid stability of cationic vesicles and bilayer-covered polystyrene microspheres.** *J Phys Chem* 1996, **100**:7130.
17. Pacheco LF, Carmona Ribeiro AM: **Effects of synthetic lipids on solubilization and colloid stability of hydrophobic drugs.** *J Coll Interface Sci* 2003, **258**:146.
18. Lentz BR: **Membrane fluidity as detected by diphenylhexatriene probes.** *Chem Phys Lipids* 1989, **50**:171.

19. Feitosa E, Barreleiro PCA, Olofsson G: **Phase transition in dioctadecyldimethylammonium bromide and chloride vesicles prepared by different methods.** *Chem Phys Lipids* 2000, **105**:201.
20. Demas JN, Crosby GA: **Measurement of photoluminescence quantum yields - Review.** *J Phys Chem* 1971, **75**:991.
21. Fery-Forgues S, Lavabre D: **Are fluorescence quantum yields so tricky to measure? A demonstration using familiar stationery products.** *J Chem Educ* 1999, **76**:1260.
22. Morris JV, Mahaney MA, Huber JR: **Fluorescence quantum yield determinations - 9,10-Diphenylanthracene as a reference-standard in different solvents.** *J Phys Chem* 1976, **80**:969.
23. Feitosa E, Brown W: **Fragment and vesicle structures in sonicated dispersions of dioctadecyldimethylammonium bromide.** *Langmuir* 1997, **13**:4810.
24. Andersson M, Hammarström L, Edwards K: **Effect of bilayer phase-transitions on vesicle structure and its influence on the kinetics of viologen reduction.** *J Phys Chem* 1995, **99**:14531.
25. Lopes A, Edwards K, Feitosa E: **Extruded vesicles of dioctadecyldimethylammonium bromide and chloride investigated by light scattering and cryogenic transmission electron microscopy.** *J Coll Interface Sci* 2008, **322**:582.
26. Valeur B: *Molecular Fluorescence - Principles and Applications*. Weinheim: Wiley-VCH; 2002.
27. Castanheira EMS, Pinto AMR, Queiroz MJRP: **Fluorescence of a benzothienopyridopyrimidone in solution and in lipid vesicles.** *J Fluorescence* 2006, **16**:251.
28. Queiroz M-JRP, Castanheira EMS, Lopes TCT, Cruz YK, Kirsch G: **Synthesis of fluorescent tetracyclic lactams by a “one pot” three steps palladium-catalyzed borylation, Suzuki coupling (BSC) and lactamization. DNA and polynucleotides binding studies.** *J Photochem Photobiol A Chem* 2007, **190**:45.
29. McGhee JD, von Hippel PH: **Theoretical aspects of DNA-protein interactions – Cooperative and non-cooperative binding of large ligands to a one-dimensional homogeneous lattice.** *J Mol Biol* 1974, **86**:469.
30. Lehrer SS: **Solute perturbation of protein fluorescence - quenching of tryptophyl fluorescence of model compounds and of lysozyme by iodide ion.** *Biochemistry* 1971, **10**:3254.
31. Papahadjopoulos D, Miller N: **Phospholipid model membranes. I. Structural characteristics of hydrated liquid crystals.** *Biochim Biophys Acta* 1967, **135**:624.

Figure 1. Structure of the compounds 1 and 2.

Figure 2. Size distributions obtained by dynamic light scattering (DLS) for DPPC, Egg-PC and DODAB liposomes prepared by the ethanolic injection method.

Figure 3. Normalized fluorescence spectra ($\lambda_{\text{exc}} = 360 \text{ nm}$) of compound 1 ($4 \times 10^{-6} \text{ M}$) in several solvents; the inset shows the absorption spectrum of 1 in dichloromethane ($1 \times 10^{-4} \text{ M}$) as an example.

Figure 4. Normalized fluorescence spectra ($\lambda_{\text{exc}} = 360$ nm) of compound **2** (4×10^{-6} M) in several solvents; the inset shows the absorption spectrum of **2** in dichloromethane (2×10^{-5} M) as an example.

Figure 5. Fluorescence spectra of compound **1** (5×10^{-6} M) in 0.01 M Tris–HCl buffer (pH = 7.2), with increasing DNA content.

Figure 6. Fluorescence spectra of compound **2** (5×10^{-6} M) in 0.01 M Tris–HCl buffer (pH = 7.2), with increasing DNA content.

Figure 7. Stern–Volmer plots for quenching with iodide ion of compounds **1** and **2** for [DNA]/[compound] = 200 (A) and corresponding modified Stern–Volmer plots (B).

Figure 8. Normalized fluorescence emission spectra of compounds **1** and **2** incorporated in liposomes of DPPC, Egg-PC and DODAB.

Table 1. Maximum absorption (λ_{abs}) and emission (λ_{em}) wavelengths, molar absorption coefficients (ϵ) and fluorescence quantum yields of compounds **1** and **2** in several solvents.

Solvent	λ_{abs} (nm) ($\epsilon/10^4 \text{ M}^{-1} \text{ cm}^{-1}$)		λ_{em} (nm)		Φ_{F}	
	1	2	1	2	1	2
Cyclohexane	398 (0.84); 377 (1.24); 360 (1.27); 305 (0.95); 258 (3.93)	411 <i>sh</i> (0.33); 354 (2.19); 347 (2.37); 308 (1.25); 291 (1.12); 270 (1.40)	402; 426; 452 <i>sh</i>	417; 441	0.20	0.047
Dioxane	398 (0.76); 377 (1.18); 359 (1.20); 305 (1.17); 258 (3.60)	411 <i>sh</i> (0.66); 356 (5.36); 346 (5.40); 309 (3.23); 291 (2.98); 272 (3.33)	407; 428; 455 <i>sh</i>	425; 449	0.29	0.054
Dichloromethane	397 (0.58); 377 (0.91); 360 (0.93); 305 (0.97); 259 (2.70)	410 <i>sh</i> (0.55); 357 (4.37); 311 (2.28); 290 (2.29); 273 (2.78)	408; 429	427; 448	0.26	0.022
Acetonitrile	395 (0.68); 376 (1.06); 358 (1.06); 304 (1.09); 256 (3.32)	409 <i>sh</i> (0.66); 355 (5.76); 308 (3.41); 289 (3.20); 271 (3.67)	408; 428	450	0.21	0.036
<i>N,N</i> -Dimethylformamide ^a	397 (0.78); 377 (1.19); 360 (1.16); 305 (1.19)	411 <i>sh</i> (0.69); 356 (5.52); 311 (3.11); 290 (2.86)	411; 430	453	0.30	0.047
Dimethylsulfoxide ^a	397 (0.77); 378 (1.17); 361 (1.14); 305 (1.17)	412 <i>sh</i> (0.61); 357 (4.70); 313 (2.52)	413; 432	455	0.28	0.048
Ethanol	396 (0.69); 375 (1.13); 358 (1.17); 304 (1.40); 256 (3.59)	408 <i>sh</i> (0.72); 355 (5.50); 311 (2.95); 272 (3.69)	412; 431	452	0.27	0.041
Methanol	395 (0.67); 374 (1.08); 358 (1.10); 304 (1.34); 256 (3.43)	408 <i>sh</i> (0.62); 354 (5.00); 311 (2.80); 272 (3.41)	413; 433	453	0.26	0.040
Water	394 (0.41); 374 (0.57); 361 (0.58); 303 (0.93); 256 (2.07)	420 <i>sh</i> (0.26); 358 (0.87); 314 (0.94); 278 (0.97)	413 <i>sh</i> ; 433	505	0.22	0.012

^aSolvent cut-offs: *N,N*-Dimethylformamide: 275 nm; Dimethylsulfoxide: 280 nm; *sh*: shoulder.

Table 2. Values of the intrinsic binding constants (K_i) and binding site sizes (n) and fraction of compound molecules accessible to external quenchers (f_a) for interaction with salmon sperm DNA.

Compound	K_i (M^{-1})	n	f_a
1	$(8.7 \pm 0.9) \times 10^3$	11 ± 3	0.89
2	$(5.9 \pm 0.6) \times 10^3$	7 ± 2	0.65

Table 3. Steady-state fluorescence anisotropy (r) values and maximum emission wavelengths (λ_{em}) of compounds 1 and 2 incorporated in liposomes.

	Compound 1		Compound 2	
	λ_{em}/nm	r	λ_{em}/nm	r
DPPC (25°C)	433	0.009	453	0.111
DPPC (55°C)	434	0.008	454	0.032
Egg-PC (25°C)	432	0.008	453	0.095
DODAB (25°C)	433	0.011	454	0.112
DODAB (55°C)	432	0.007	455	0.051
Glycerol (25°C)	437	0.166	472	0.202

Values in glycerol are also shown for comparison.

FIGURES

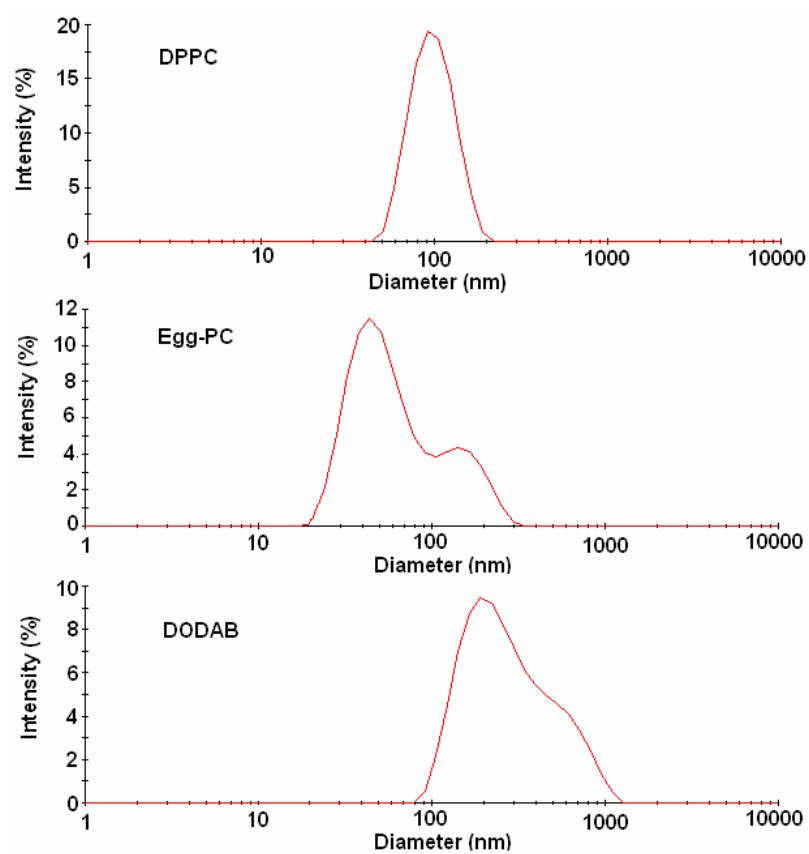
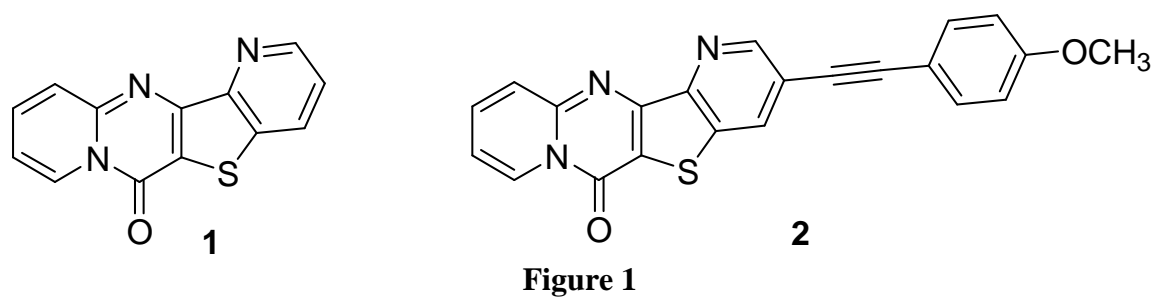


Figure 2

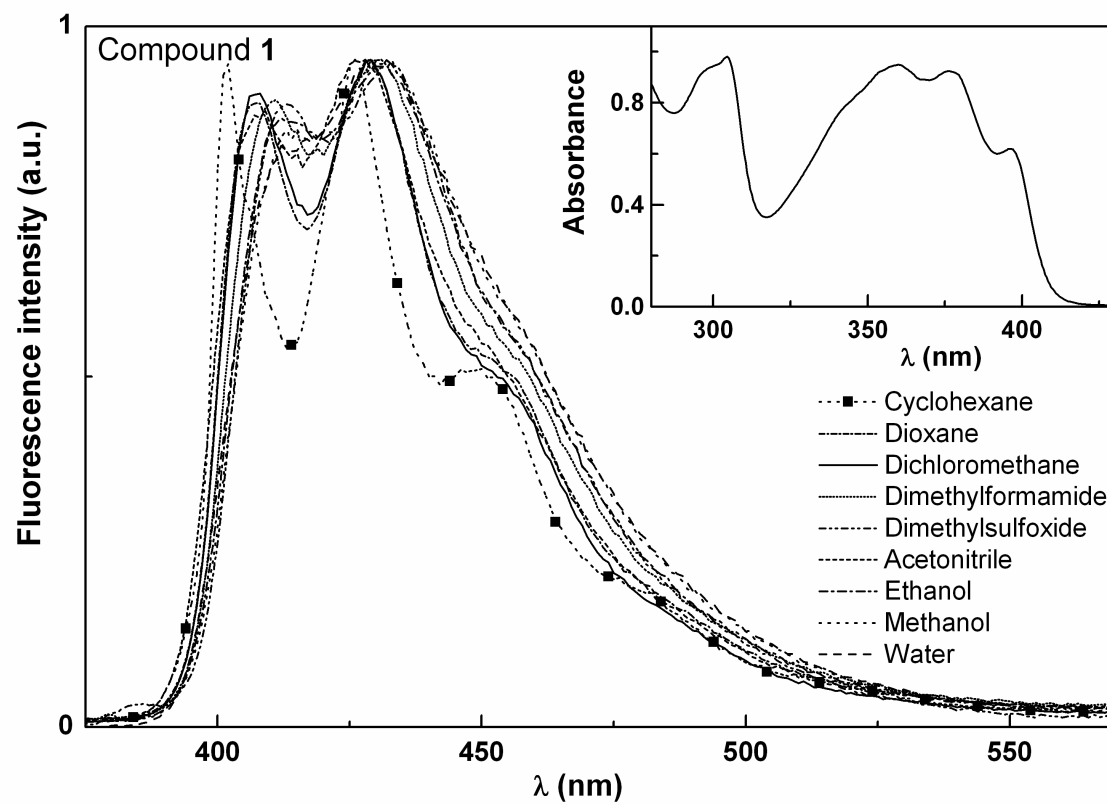


Figure 3

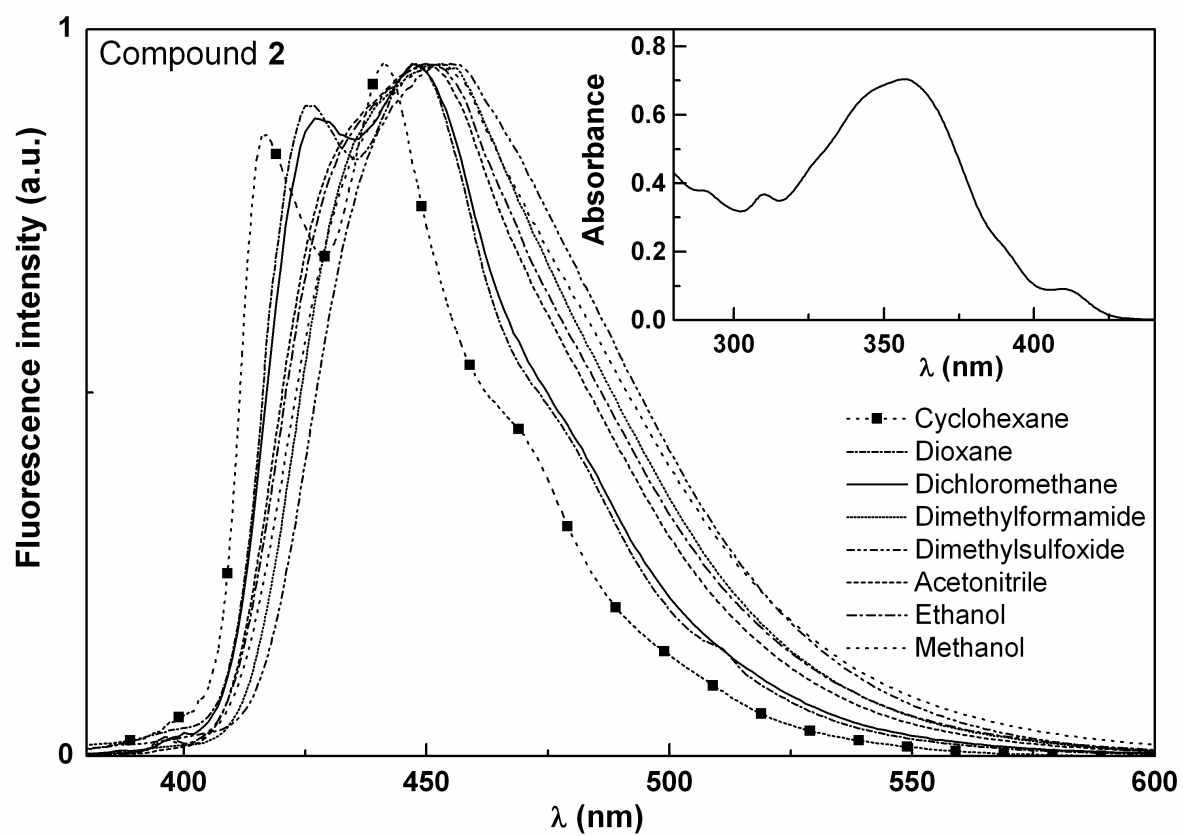


Figure 4

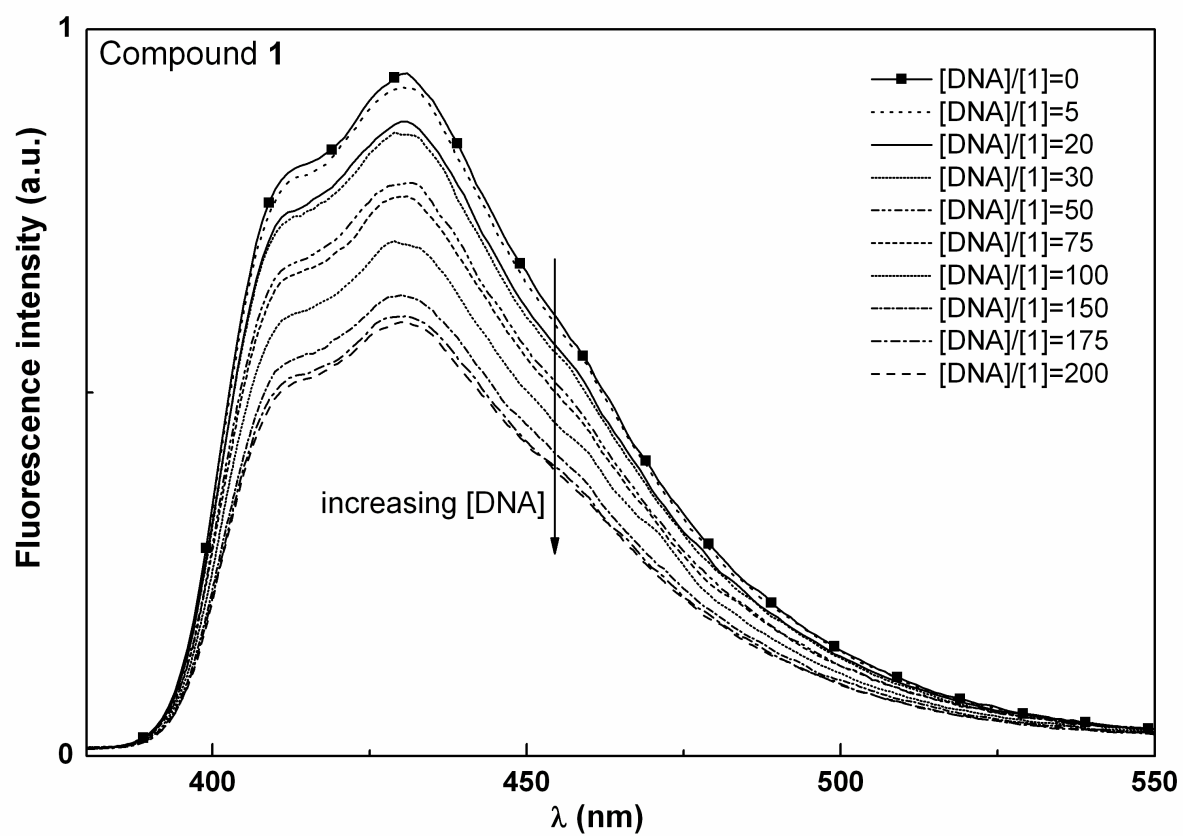


Figure 5

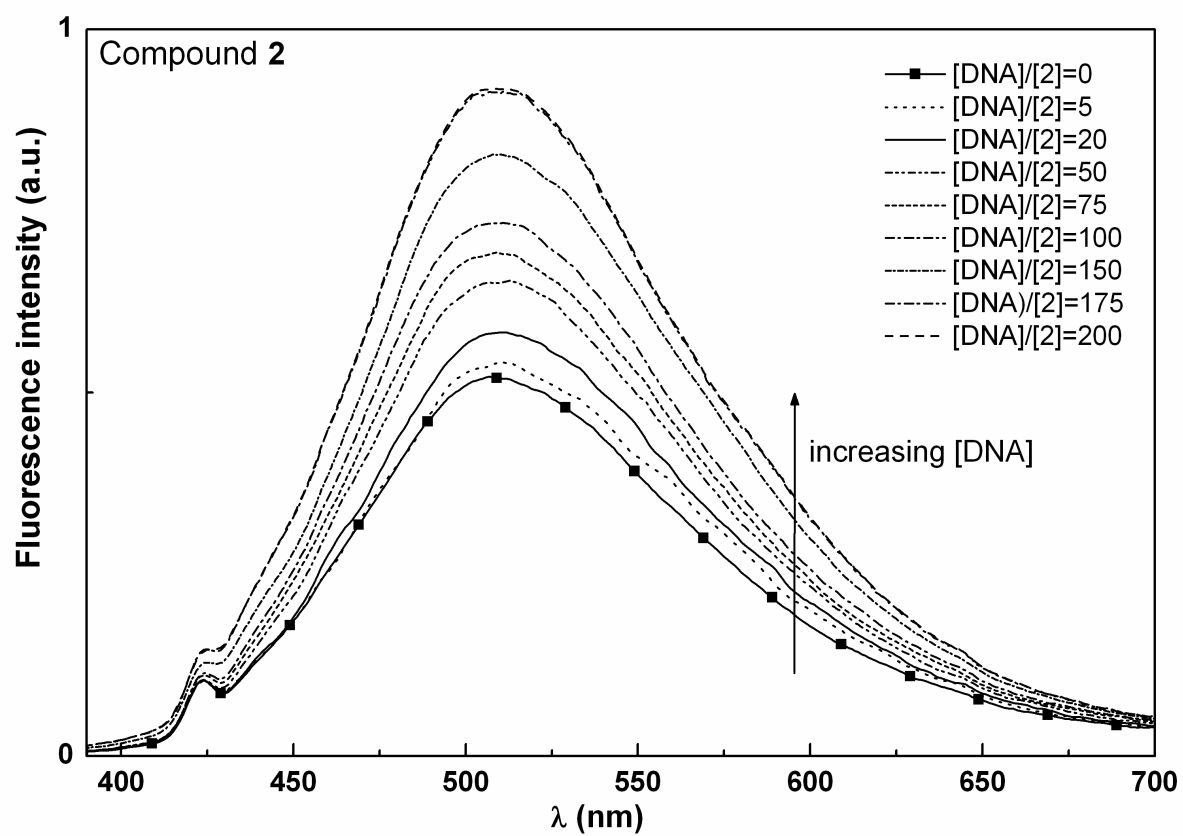


Figure 6

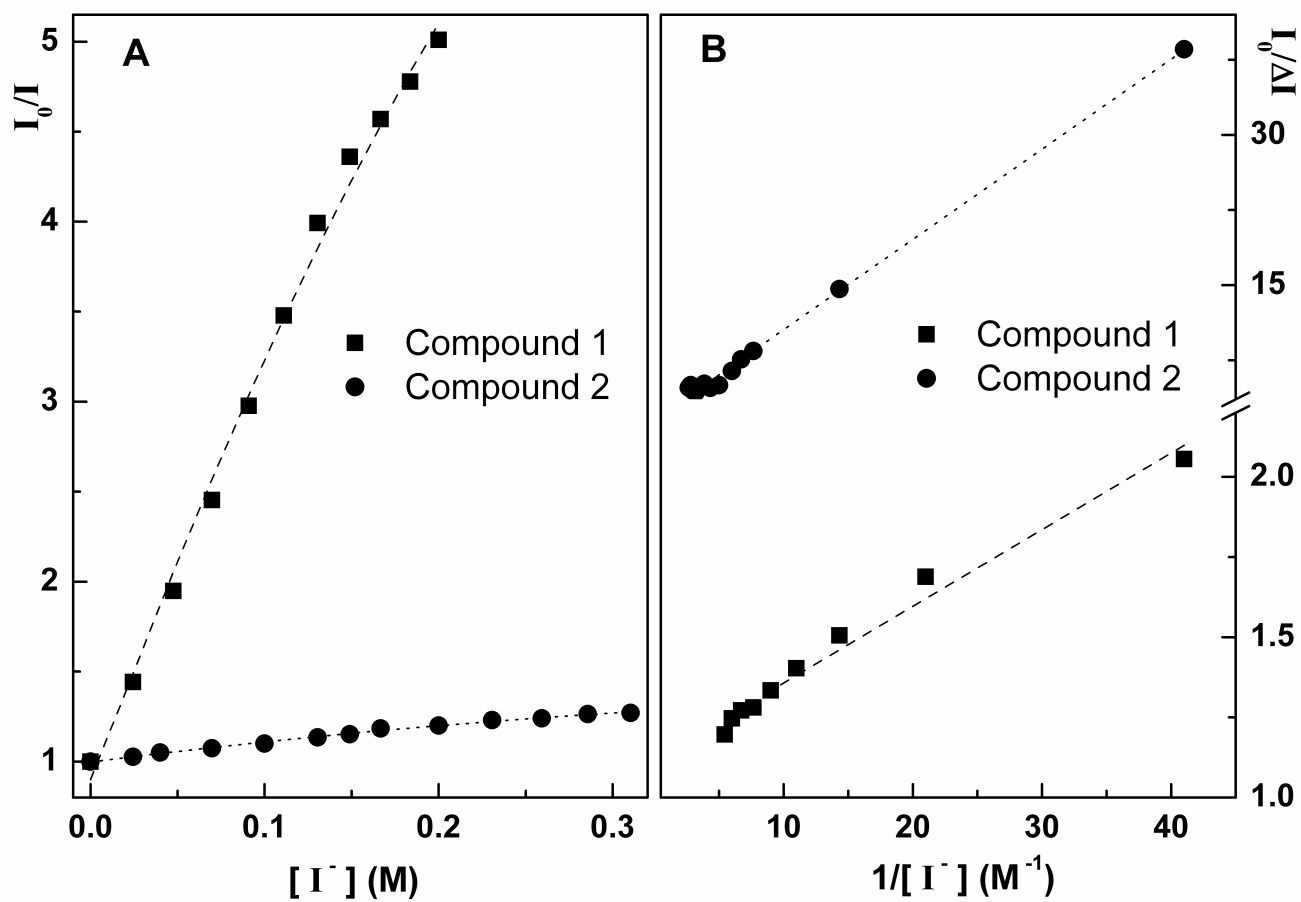


Figure 7

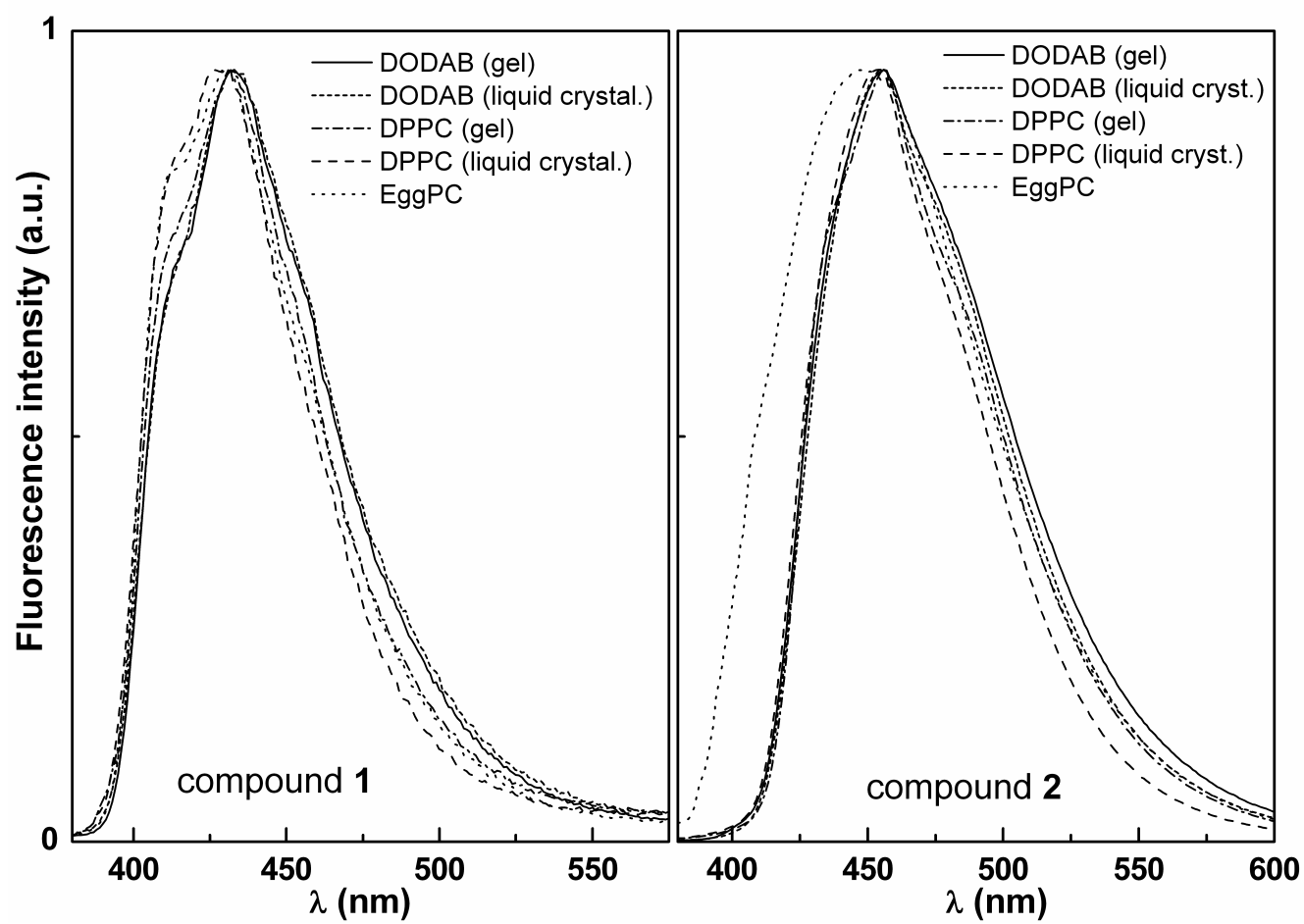


Figure 8